

CONF-8806225--2
2001-55-6.2.25-2
MOMENTUM DISTRIBUTIONS OF NEUTRAL PIONS
IN HEAVY ION REACTIONS AT THE CERN - SPS ¹

WA80 COLLABORATION

CONF-8806225--2

DE89 003181

H. Löhner^{d,f}, R. Albrecht^a, T. C. Awes^c, C. Baktash^c, P. Beckmann^d, F. Berger^d,
R. Bock^a, G. Claesson^a, L. Dragon^d, R. L. Ferguson^c, A. Franz^b, S. Garpman^c,
R. Glasow^d, H. A. Gustafsson^c, H. H. Gutbrod^a, K. H. Kampert^{d,g}, B. W. Kolb^a,
P. Kristiansson^b, I. Y. Lee^c, I. Lund^{a,h}, F. E. Obenshain^{e,i}, A. Oskarsson^c,
I. Otterlund^c, T. Peitzmann^d, S. Persson^c, F. Plasil^c, A. M. Poskanzer^b,
M. Purschke^d, H. G. Ritter^b, R. Santo^d, H. R. Schmidt^a, T. Siemarczuk^{a,j},
S. P. Sorensen^{e,i}, E. Stenlund^c, and G. R. Young^c

1101
1121
1131
1141
1151
1161
1171
1181
1191
1201
1211
1221
1231
1241
1251
1261
1271
1281

- a. Gesellschaft für Schwerionenforschung (GSI), D-6100 Darmstadt
- b. Lawrence Berkeley Laboratory, Berkeley, California 94720, USA
- c. University of Lund, S-22362 Lund
- d. University of Münster, D-4400 Münster
- e. Oak Ridge National Laboratory, Oak Ridge, Tennessee 37831, USA
- f. present address: KVI, University of Groningen, NL-9747 AA Groningen
- g. Post Doctoral Fellowship from the German Research Community (DFG)
- h. Post Doctoral Fellowship from Swedish Natural Research Science Council
- i. University of Tennessee, Knoxville, Tennessee 37996, USA
- j. On leave of absence from the Inst. of Nuclear Studies, PL-00681 Warsaw

1. INTRODUCTION

A systematic study of nucleus+nucleus reactions at ultrarelativistic energies has been started in 1986 with oxygen beams of 60 and 200 A-GeV in the CERN-SPS in order to investigate nuclear matter under extreme conditions of density and excitation energy. According to QCD lattice calculations^{/1} a first or second order transition to the deconfined phase of quarks and gluons, the quark-gluon-plasma (QGP), may occur in a finite volume of hadronic matter at energy densities larger than the energy density inside the nucleon^{/2}. First experimental results from ¹⁶C + nucleus reactions^{/3,4/} show that, in the most central events, energy densities above 2 GeV/fm³ are reached. Up to now, cosmic ray data have been the only source of information^{/5/} and the observed rise of their transverse momenta with energy density has been interpreted as due to QGP effects^{/6/}. Since the signature of the QGP is not well established, p + nucleus data have been taken for comparison to the nucleus+nucleus data at the same incident energy per nucleon in order to observe in the heavy ion induced reactions any deviation in the distribution of transverse momenta.

Invited talk presented at the
IX. International Seminar on High Energy Physics Problems
Relativistic Nuclear Physics and Quantum Chromodynamics
Dubna (USSR), 14 - 19 June, 1988

M. STER

2. EXPERIMENT

The WA80 experiment at the CERN-SPS is designed to measure the distribution of charged particles in a large fraction of phase space, to analyse the forward and transverse energy distributions and to investigate the target fragmentation region. In addition, photons and neutral pions are identified near midrapidity in a high resolution lead glass calorimeter. This allows a detailed analysis of their transverse momenta (p_T) based on centrality selections which are determined either by measurements of the remaining projectile energy in the forward direction or the charged particle multiplicity. The experimental setup is described in detail in ref.^{/7/}. The results presented in this paper were derived from the following detector components: the electromagnetic lead glass calorimeter (SAPHIR), the uranium scintillator sampling calorimeter at zero degree (ZDC), and the streamer tube multiplicity arrays which cover the pseudorapidity region $1.2 \leq \eta \leq 4.2$.

SAPHIR measures the inclusive photon and π^0 distributions at midrapidity with a pseudorapidity coverage of $1.5 \leq \eta \leq 2.1$ and a solid angle of 0.13 steradian. Details of the construction and performance are given in ref.^{/8/}. The streamer tube material contributes 4 % to the photon conversion probability. The target vacuum chamber contributes an additional 0.4 %. Background levels during target-out operation were found negligible.

The ZDC characterizes the centrality of each collision by measuring the remaining energy of projectile spectators for lab. angles $\leq 0.3^\circ$. A strong correlation between charged particle multiplicity and energy in ZDC is observed^{/9/}, so that either quantity may be used to distinguish between peripheral and central reactions.

3. PHOTON DISTRIBUTIONS

Inclusive spectra of photons, which dominantly originate from π^0 decay, have been extracted from the raw data applying selection criteria based upon the electromagnetic shower development in the lead glass and the multiplicity detectors in front^{/8/}. Systematic errors originating in misidentification are included in the error bars shown in the photon spectra.

Fig. 1 shows inclusive photon p_T spectra containing about 10 % of the minimum bias cross section after a selection of events with high charged particle multiplicity. The data are described by an exponential parametrization

$$dN/dp_T \sim \exp(-p_T/T_{\text{eff}}) \text{ for } p_T > 0.4 \text{ GeV/c.} \quad (1)$$

The slope parameters T_{eff} increase slightly with increasing target- and projectile-mass and incident energy. The experimental data are compared with the Lund model FRITIOF^{/10/} for nucleus+nucleus interactions. The predicted inverse slopes are in general about 20 % lower than the slope parameters fitted to the data.

In order to investigate the p_T distributions in more detail with respect to their centrality dependence, ratios of oxygen cross sections for a heavy ($^{16}\text{O} + \text{Au}$) and a light ($^{16}\text{O} + \text{C}$) target have been calculated and are presented in fig. 2 as a function of p_T for the 10 % most central and the 10 % most peripheral reactions as defined from the charged particle multiplicity. For central collisions an increase of this ratio by a factor of 2 is observed between $p_T = 0.2$ GeV/c and 2 GeV/c whereas in peripheral collisions almost no dependence on p_T is visible. We conclude, that large transverse momenta are produced more efficiently in violent (central) reactions and large interacting systems, i.e. target-projectile overlap volumes. The FRITIOF model, containing the basic kinematical constraints, does not exhibit any different slope of p_T distributions for central and peripheral reactions or for different target masses and is in this respect consistent only with the most peripheral data sample.

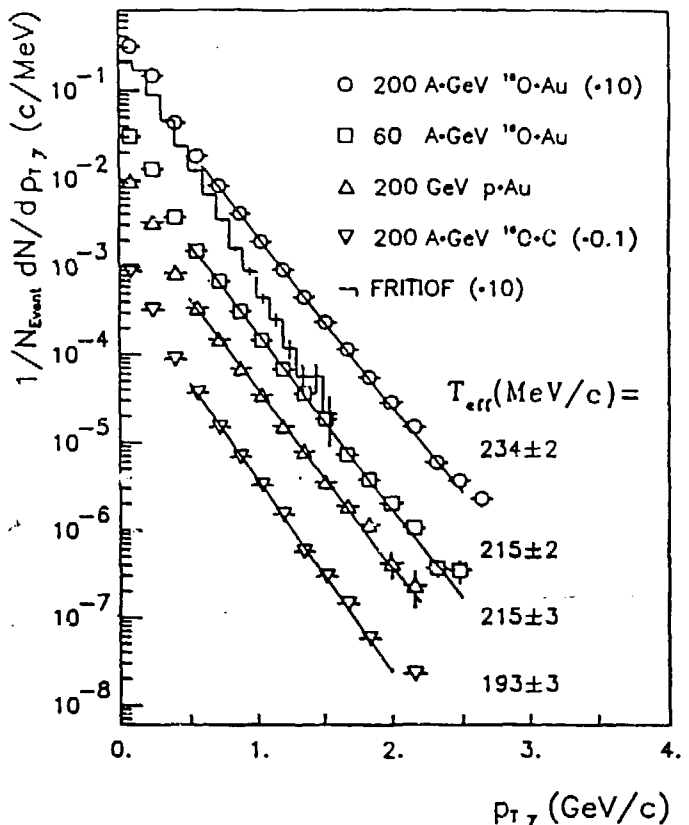


Figure 1: Inclusive photon p_T distributions from proton and oxygen induced reactions at 200 and 60 A-GeV measured in $1.5 \leq \eta \leq 2.1$. Central reactions are selected with 10 % of the minimum bias cross section. For comparison with exponential parametrizations (solid lines) the histogram shows the FRITIOF model results for $^{16}\text{O} + \text{Au}$ at 200 A-GeV.

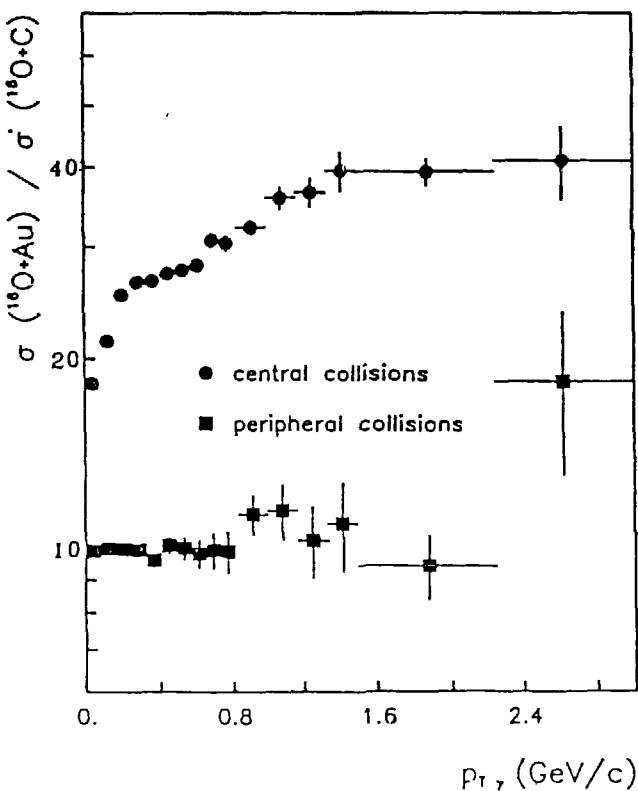


Figure 2: Ratios of inclusive photon cross sections for $^{16}\text{O} + \text{Au}$ and $^{16}\text{O} + \text{C}$ reactions at 200 A-GeV. The selections according to the charged particle multiplicity contain the 10 % most central (upper part) and the 10 % most peripheral reactions (lower part), respectively.

Since the deviation from FRITIOF is significant for $p_T > 0.4$ GeV/c in the photon distributions, we have analyzed the p_T region above 0.4 GeV/c as a function of target mass and event centrality in a model independent way by computing algebraically the average p_T from distributions cut off at a lower p_T value C :

$$\langle p_T \rangle_{\gamma,C} = \left(\int_C^\infty p_T \frac{dN}{dp_T} dp_T / \int_C^\infty \frac{dN}{dp_T} dp_T \right) - C, \quad (2)$$

using $C = 400$ MeV/c. The resulting $\langle p_T \rangle_{\gamma,C}$ is equal to the slope parameter T_{eff} for a purely exponential distribution in the region $p_T > C$.

In order to compare the oxygen and proton induced reactions properly for different degrees of centrality and to relate the obtained $\langle p_T \rangle_{\gamma,C}$ values to thermodynamical models^{11/}, we have introduced the variable S proportional to the entropy density^{11,12/}: $S = (dN/d\eta) \cdot A_{\text{inc}}^{-2/3}$. Here $(dN/d\eta)$ is the central multiplicity density which is approximated by the charged particle multiplicity in $1.2 \leq \eta \leq 4.2$ multiplied by 1.5 in order to correct for undetected neutral particles. A_{inc} is the mass number of the smaller colliding nucleus in central collisions. For peripheral heavy ion collisions, however, this assumption is no longer justified. Therefore A_{inc} is defined to be the number of incident projectile participants, which is derived from the ZDC energy via the FRITIOF model in close resemblance to ref.^{14/}. In this way the oxygen data are expected to correspond to the proton data for very low values of the entropy density. The resulting $\langle p_T \rangle_{\gamma,400}$ of photons is plotted as a function of the entropy density in fig. 3. The data points at highest S contain 10 % of the minimum bias cross section. Their $\langle p_T \rangle_{\gamma,400}$ increases gradually for growing size of the target-projectile overlap for $^{16}\text{O} + \text{C}$ via $\text{p} + \text{Au}$ to $^{16}\text{O} + \text{Au}$ at the same incident energy and also increases with increasing beam energy. A remarkable feature of fig. 3 is the reduced increase of $\langle p_T \rangle_{\gamma,400}$ at intermediate and large values of the entropy density S for $^{16}\text{O} + \text{Au}$ reactions at 200 A-GeV. At low entropy density the rise of $\langle p_T \rangle_{\gamma,400}$ may even become steeper by up to 6 % due to possible systematic errors in the photon identification. Thus, the deviation from FRITIOF is obvious, since this model predicts almost no variation with centrality or target mass. Although, it has to be noted, that in the present FRITIOF version hard scattering^{13/} is not yet included for nucleus+nucleus reactions. However, preliminary investigations^{14,15/} seem to indicate that only a small fraction of the observed effect can be explained in this way. On the other hand, a structure like this is expected from thermodynamical and hydrodynamical studies^{11,16,17/} of the QGP phase transition and is reminiscent of earlier observations of cosmic ray data^{5/}. The relative variation of $\langle p_T \rangle_{\gamma,400}$ for $\text{p} + \text{Au}$ at 200 GeV (fig. 3) is consistent with data obtained from $\text{p} + \text{p}$ and $\alpha + \alpha$ reactions at the ISR^{18/}. The increase to larger values of $\langle p_T \rangle$ in $\text{p} + \bar{\text{p}}$ collider data^{19/}, where equivalently large entropy values are reached, is more closely resembling the $^{16}\text{O} + \text{Au}$ data than the $\text{p} + \text{Au}$ data.

4. π^0 DISTRIBUTIONS

The momentum distributions of inclusive photons analysed in the previous section allow studies of the centrality dependence for different reaction systems with good statistical accuracy. From the various sources (π^0 and η^0 mesons, baryon resonances) contributing photons to the observed distributions, the π^0 are clearly dominating and expected to influence the results most strongly. However, the reaction kinematics and possible changes in the effective center of mass (CM) system make it difficult to extract absolute numbers of average transverse momenta for π^0 from inclusive photons. Therefore, cross sections for π^0 production and their p_T distributions have been obtained by analysing the invariant mass spectra of $\gamma\gamma$ pairs in small intervals of p_T .

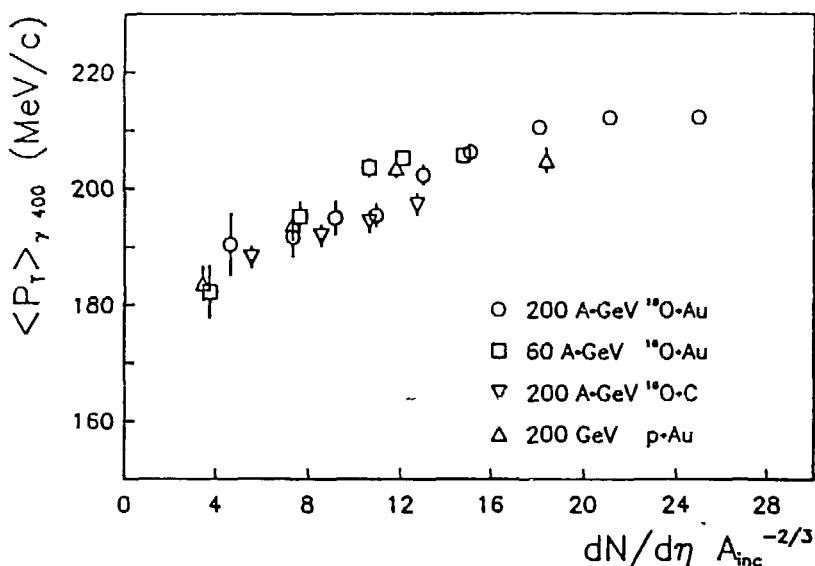


Figure 3: Experimental $\langle p_T \rangle_{\gamma,400}$ for inclusive photons from the truncated p_T distribution (see text) as function of the entropy density estimated from the central charged particle multiplicity and the number of participating projectile nucleons which is calculated from the energy in the ZDC.

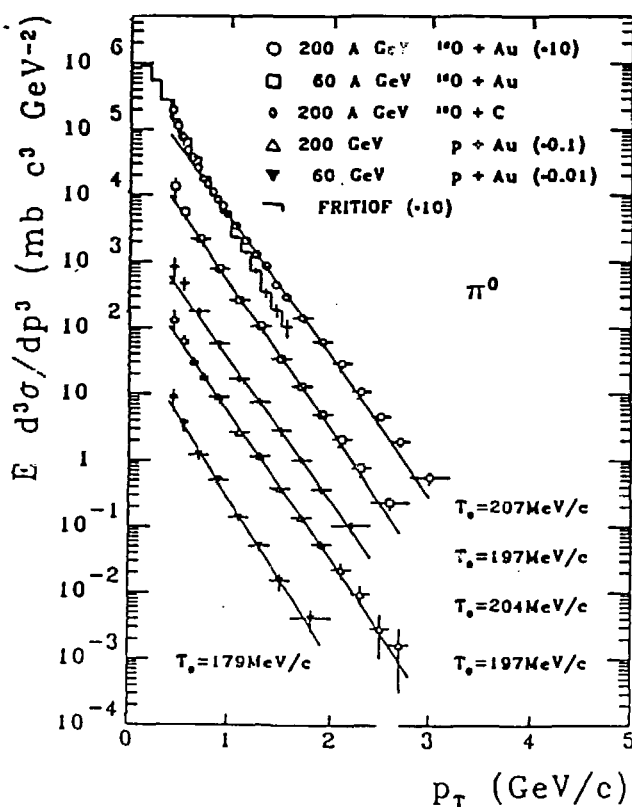


Figure 4: Invariant cross sections for π^0 as a function of p_T from proton and oxygen induced reactions at 200 and 60 A-GeV measured in $1.5 \leq \eta \leq 2.1$ for different target masses. For comparison with exponential parametrizations (solid lines) the histogram shows the FRITIOF model results for $^{16}\text{O} + \text{Au}$ at 200 A-GeV.

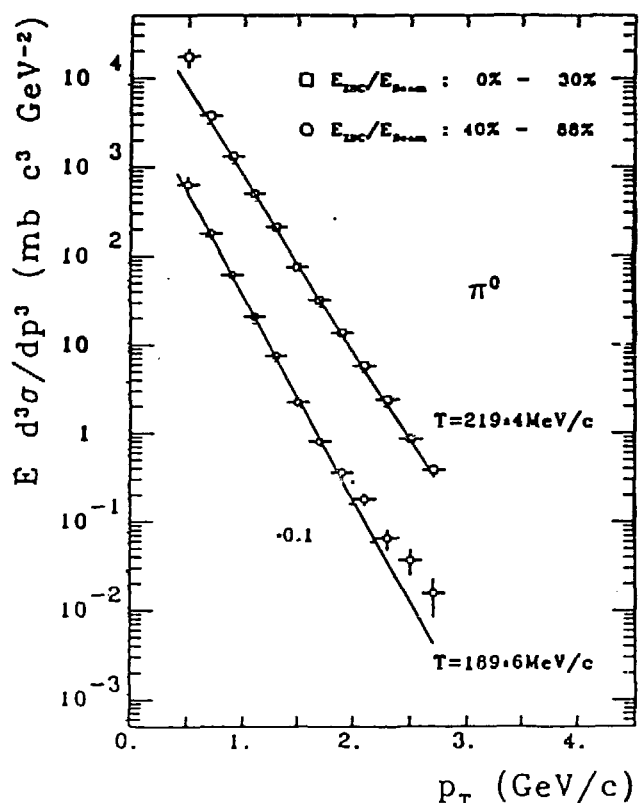


Figure 5: Invariant cross sections for π^0 as a function of p_T from oxygen induced reactions at 200 A-GeV measured in $1.5 \leq \eta \leq 2.1$ for the 40 % most central and the 50 % most peripheral reactions as selected by the energy measured in ZDC.

The obtained π^0 cross sections from $p + \text{Au}$ reactions are consistent with Fermilab data^{/20/} within the error limits for π^+ and π^- from $p + \text{W}$ at 200 GeV incident energy and in approximately the same region of rapidity. Furthermore, π^0 distributions have been studied in different regions of pseudorapidity within the acceptance of SAPHIR ranging from 1.5 to 2.1 units in η . From this we conclude that at most a variation of $(6 \pm 4)\%$ in the slope of p_T distributions might originate from a change in the effective CM system when central and peripheral ^{16}O induced reactions are compared.

In fig. 4 the p_T dependence of invariant π^0 cross sections for minimum bias trigger conditions from proton and oxygen induced reactions is compared for different targets and energies. The slopes of these distributions can be described by an exponential parametrization

$$1/p_T \, dN/dp_T \sim \exp(-p_T/T_0). \quad (3)$$

Slope parameters T_0 have been deduced from the same restricted transverse momentum range $0.8 \text{ GeV}/c \leq p_T \leq 2 \text{ GeV}/c$ for all reaction systems. These parameters turn out to be similar for proton and oxygen induced reactions in these minimum bias data and are only weakly dependent on target mass, but are larger by at least 20% for $^{16}\text{O} + \text{Au}$ at 200 A-GeV than for $p + p$ reactions^{/21/} and for FRITIOF model predictions. This behaviour is consistent with the observations cited above which show that the linear extrapolation from $p + p$ reactions to heavy ion reactions, as contained in this model, is doubtful. The deviation from FRITIOF by a factor of 3 at $p_T = 1.5 \text{ GeV}/c$ may hardly be explained by multiple hard scattering since this effect produces only a 30% increase in calculations^{/14/} of $p + p$ reactions at ISR energies.

The spectra in fig. 4 indicate a change in slope below $p_T \approx 0.8 \text{ GeV}/c$, which is most pronounced for the heavy system. A slope parameter $T_0 \leq 150 \text{ MeV}/c$ would be appropriate to describe the data for $p_T < 0.8 \text{ GeV}/c$. This effect is not seen in 250 GeV/c $p + p$ reactions^{/21/}, but is consistent with $\alpha + \alpha$ reactions at the ISR^{/18,22,23/} and weakly indicated in the $p + \text{Au}$ data at 200 GeV. This feature is also predicted in thermodynamical models^{/17,24/} and in studies of the hydrodynamical expansion^{/16,25/} of hot hadronic systems.

Further details of the pion momentum distributions are revealed by inspecting their dependence on the impact parameter. Fig. 5 shows two distributions for the 40% most central and the 50% most peripheral reactions as selected by the energy measured in ZDC relatively to the beam energy. The exponential curves (equ. 3) fit the data in the region $0.8 \leq p_T \leq 2 \text{ GeV}/c$ with slope parameters increasing by $\approx 15\%$ with increasing centrality as expected from the previous inclusive photon analysis. Deviations from a single exponential curve at low p_T for central data and at high p_T for peripheral data, which suggest a hard component, demand a systematic investigation as presented for example in fig. 6, inspired by a similar analysis performed for $\alpha + \alpha$ and $p + p$ reactions at ISR energies^{/22/}. $R_{\text{ZDC}}(p_T)$ is the ratio of the ZDC-selected dN/dp_T distribution relative to the minimum bias distribution, while each distribution is normalized to unity. Here again the degree of centrality increases with decreasing energy in ZDC. We observe in complete analogy to ref.^{/22/} that the bump at low p_T (0.8 GeV/c) for peripheral data (low multiplicity) changes to a dip for central (high multiplicity) selection. This behaviour again shows the difficulty in interpreting a single number like the average p_T taken over the full p_T range, because it washes out any structure in the p_T dependence, which might contain essential dynamical information.

The π^0 analysis underlines the previous findings that the tails of the p_T distributions measured in midrapidity are enhanced beyond $p_T = 0.8 \text{ GeV}/c$ for high particle density or central collisions in close resemblance to hadron+hadron^{/21/} or $\alpha + \alpha$ reactions^{/22/} at total CM energies between 22 and 62 GeV. There, however, the enhancement appears already for $p_T > 0.4 \text{ GeV}/c$ and is of the order of $\approx 5\%$ in magnitude. In the $^{16}\text{O} + \text{Au}$ case at 19.4 GeV total energy in the

nucleon-nucleon CM system we observe an effect of 15 %, which only in part can be explained by a variation of the effective CM system, though.

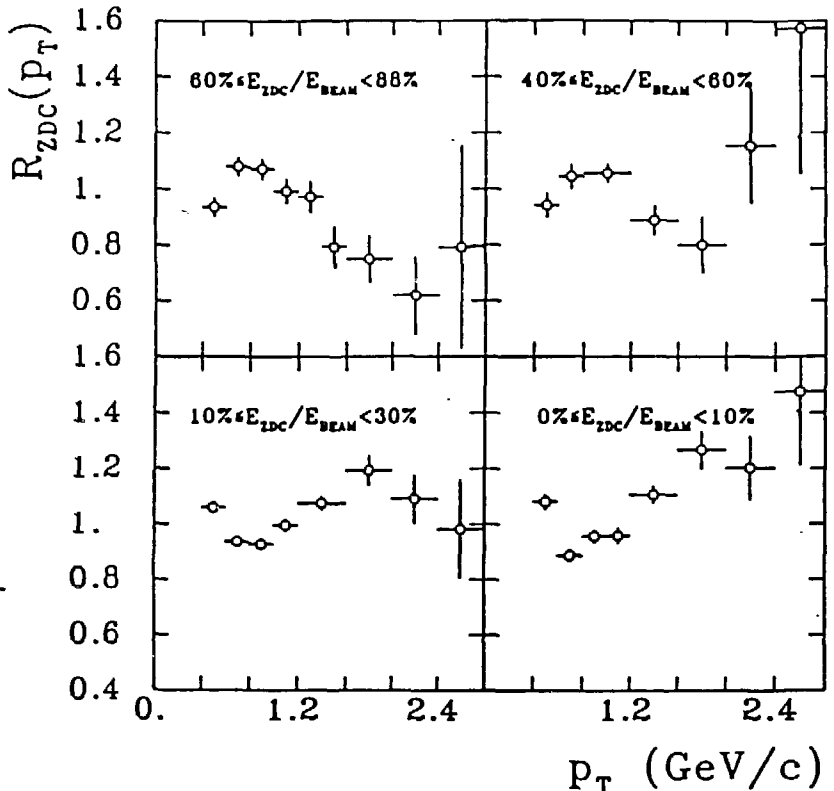


Figure 6: Ratios of ZDC-selected π^0 distributions relative to the minimum bias distribution for $^{16}\text{O} + \text{Au}$ at 200 A-GeV as a function of p_T .

5. η^0 MESONS AND SINGLE PHOTONS

Besides the investigation of pion momentum distributions and correlation studies, the ultimate objective of photon detection in heavy ion collisions has been the detection of direct photons which promise to give a clean signal^{/26,27/} for the expected quark gluon plasma. This analysis, however, is severely hampered by the presence of decay photons from various meson decays. Among those the π^0 and η^0 mesons are clearly the dominating source of single photon background. It is therefore necessary to determine the η^0/π^0 production ratio in the same experiment. Due to the larger opening angle for the η^0 decay photons, the acceptance of our detector^{/8/} is much lower than for π^0 . Nevertheless we obtain the mass spectrum shown in fig. 7 where a clear η^0 signal in a limited p_T region is observed with an η^0 peak width compatible with the detector resolution. We derive the ratio $\eta^0/\pi^0 = 0.74 \pm 0.23$ which is in accordance with the result of $\eta^0/\pi^0 = 0.45 \pm 0.10$ from $p + p$ reactions^{/28/} at 63 GeV total CM energy. Thus with the quite reasonable assumption of m_T scaling for η^0 and π^0 we are able to compute their contribution to the inclusive photon distribution. Heavier mesons are expected to produce only an additional small fraction of the η^0 contribution^{/29/}.

Thus, we are now able to compute the photon/ π^0 ratio as a function of p_T and to subtract the photon/ π^0 distribution obtained from the measured meson distributions. From the observed difference spectrum we conclude that in the region $1 \leq p_T \leq 2.5$ GeV/c the goal of a 5 % detection level as determined by the error bars can be reached. In this region a remarkable enhancement of about 10 % appears above a distribution rising slowly from 0 to about 25 % at $p_T = 3$ GeV/c. A smooth distribution of the latter type would be expected from earlier direct photon studies^{/29/}. A thorough analysis of all possible sources of systematic errors is currently under way in order to confirm the apparent photon enhancement.

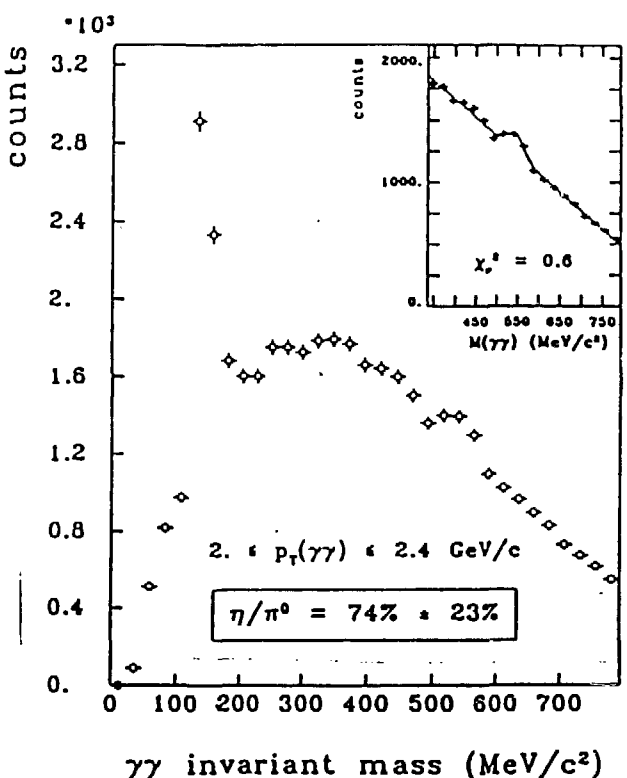


Figure 7: Invariant mass spectra of $\gamma\gamma$ pairs for $^{16}\text{O} + \text{Au}$ at 200 A-GeV. Only photons with $E_\gamma > 500 \text{ MeV}$ and $2 \text{ GeV}/c \leq p_{T,\gamma\gamma} \leq 2.4 \text{ GeV}/c$ are considered. The inset shows the polynomial fit to the combinatorial background and the gaussian η^0 mass peak with 3 % (σ) mass resolution.

6. CONCLUSIONS

In summary, it has been shown that even in the high multiplicity environment of $^{16}\text{O} + \text{Au}$ reactions the identification of π^0 in the invariant mass spectrum of $\gamma\gamma$ pairs is achieved with good accuracy in a lead glass detector. Inclusive photon spectra and p_T distributions for identified π^0 have been presented for 60 and 200 A-GeV $^{16}\text{O} +$ nucleus and $p +$ nucleus reactions.

The photon spectra show in the region $p_T > 0.4 \text{ GeV}/c$ a target mass and centrality dependence which is not predicted by the current FRITIOF model. Reactions with different initial geometry can be compared with each other when $\langle p_T \rangle$ is plotted as a function of entropy density calculated from the multiplicity and the number of projectile participants. The leveling off of a purely linear increase of $\langle p_T \rangle_{7,400}$ with entropy density for $^{16}\text{O} + \text{Au}$ at 200 A-GeV reveals a behaviour expected in the presence of a phase transition.

The π^0 p_T distributions show at least two components, a low p_T one with an inverse slope of about 150 MeV/c and a high p_T component with a flatter slope dependent slightly on target mass. These features are not compatible with a FRITIOF type linear extrapolation from $p + p$ data to heavy ion reactions. A description in terms of a thermodynamical evolution and hydrodynamical expansion of a hot hadronic system seems to be justified and has to be pursued in the future for quantitative comparisons. Nevertheless, hard scattering of partons needs to

be included in nucleus+nucleus interaction models, in order to study if the above observations can be explained within refined non-thermal models. Finally, investigations of π^0 correlations and η^0/π^0 ratios as well as direct photon production have been started and show reasonable results. Their analysis still needs more elaborate work but will soon provide an efficient number of observables to compare hadron+hadron, hadron+nucleus and nucleus+nucleus reactions and trace their similarities as well as their differences.

This work is partially supported by the West German BMFT and DFG, the VW-Stiftung, the United States DOE, the Swedish NFR and the Humboldt Foundation.

References

1. L. McLerran and B. Svetitsky, Phys. Lett. B 98 (1981) 195;
T. Celik, J. Engels and H. Satz, Nucl. Phys. B 256 (1985) 670
2. Jacob and H. Satz (eds.), *Quark Matter Formation and Heavy Ion Collisions*,
Proceedings of the Bielefeld Workshop, May 1982 (World Scientific Publ. Co., 1982)
3. A. Bamberger et al., Phys. Lett. B 184 (1987) 271
4. R. Albrecht et al., WA80 collaboration, Phys. Lett. B 199 (1987) 297
5. T. H. Burnett et al., Phys. Rev. Lett. 57 (1986) 3249
6. E.V. Shuryak and O.V. Zhirov, Phys. Lett. B 171 (1986) 99
7. H.H. Gutbrod et al., GSI preprint GSI-85-32, August 1985 and CERN SPSC/85 - 39/M406
8. H. Löhner et al., WA80 collaboration, Z. Phys. C 38 (1988) 97;
R. Albrecht et al., WA80 Collaboration, Phys. Lett. B 201 (1988) 390
9. I. Lund et al., WA80 collaboration, Z. Phys. C 38 (1988) 51
10. B. Nilsson-Almqvist and E. Stenlund, Computer Physics Com. 43 (1987) 387
11. L. Van Hove, Nucl. Phys. A 447 (1985) 443c
12. J. D. Bjorken, Phys. Rev. D 27 (1983) 140
13. M. Lev and B. Petersson, Z. Physik C 21 (1983) 155
14. B. Nilsson-Almqvist, proceedings of the *International Europhysics Conference on High Energy Physics*, Uppsala, Sweden, 1987, volume I, p. 481
15. E. Stenlund, private communication
16. M. Kataja et al., Phys. Rev. D 34 (1986) 2755
17. E. V. Shuryak, Phys. Rep. 61 (1980) 71
18. A. Breakstone et al., Phys. Lett. B 183 (1987) 227
19. G. Arnison et al., Phys. Lett. B 118 (1982) 167;
T. Alexopoulos et al., Phys. Rev. Lett. 60 (1988) 1622
20. D. Antreasyan et al., Phys. Rev. D 19 (1979) 764
21. P.A. van Hal, NA22 collaboration, Thesis, University of Nijmegen 1987
22. W. Bell et al., Z. Phys. C 27, 191 (1985)
23. A.L.S. Angelis et al. Phys. Lett. B 185 (1987) 213
24. M. Danos and J. Rafelski, Phys. Rev. D 27 (1983) 671
25. J. P. Blaizot and J. Ollitrault, Phys. Lett. B 191 (1987) 21
26. R.C. Hwa and K. Kajantie, Phys. Rev. D 32 (1985) 1109
27. S. Raha and B. Sinha, Phys. Rev. Lett. 58 (1987) 101
28. T. Akesson et al., Phys. Lett. B 178 (1986) 447
29. M. Diakonou et al., Phys. Lett. B 91 (1980) 296

DISCLAIMER

This report was prepared as an account of work sponsored by an agency of the United States Government. Neither the United States Government nor any agency thereof, nor any of their employees, makes any warranty, express or implied, or assumes any legal liability or responsibility for the accuracy, completeness, or usefulness of any information, apparatus, product, or process disclosed, or represents that its use would not infringe privately owned rights. Reference herein to any specific commercial product, process, or service by trade name, trademark, manufacturer, or otherwise does not necessarily constitute or imply its endorsement, recommendation, or favoring by the United States Government or any agency thereof. The views and opinions of authors expressed herein do not necessarily state or reflect those of the United States Government or any agency thereof.